https://doi.org/10.15407/ujpe70.2.99

L.A. BULAVIN,[1,2] YU.L. ZABULONOV,[3] P. KOPCANSKY,[4] YE.G. RUDNIKOV[1,5]

[1] Taras Shevchenko National University of Kyiv
(64/13, Volodymyrska Str., Kyiv 01601, Ukraine)
[2] Institute for Safety Problems of Nuclear Power Plants, Nft. Acad. Sci. of Ukraine
(12, Lysohirska Str., 12, Kyiv 03028, Ukraine; e-mail: bulavin221@gmail.com)
[3] Institute of Environmental Geochemistry, Nat. Acad. Sci. of Ukraine
(34a, Akademika Palladina Ave., Kyiv 03142, Ukraine)
[4] Institute of Experimental Physics, Slovak Academy of Sciences
(47, Watsonova Str., Košice 04001, Slovak Republic)
[5] National Technical University of Ukraine "Igor Sikorsky Kyiv Polytechnic Institute"
(37, Beresteiskyi Ave., Kyiv 03056, Ukraine; e-mail: erudni67@gmail.com)

COMPARATIVE ANALYSIS OF THE TEMPERATURE DEPENDENCE OF ADIABATIC THERMODYNAMIC COEFFICIENTS OF LIQUID H_2O, H_2O_2, AND Ar

Temperature dependences of the adiabatic thermodynamic coefficients of water, where the network of hydrogen bonds is formed under certain conditions, have been compared with the corresponding dependences for hydrogen peroxide, where hydrogen bonds do exist, but the network of hydrogen bonds does not, and for argon with no hydrogen bonds at all. In our opinion, specific temperature dependences of the indicated parameters for water are associated with the existence of a network of hydrogen bonds in water under certain conditions. This network is formed by two dynamic structures (the LWD and HDW phases) and is responsible for the hierarchy of anomalous water properties in a wide temperature interval. In addition, it has been shown that the network of hydrogen bonds substantially affects the behavior of the temperature dependence of the sound propagation speed related to the adiabatic coefficient of liquid compressibility.

Keywords: water, argon, hydrogen peroxide, adiabatic compressibility coefficient, sound speed, hydrogen bonds.

1. Introduction

Water is one of the most complicated liquids in nature by its properties [1, 2]. Water demonstrates the unique behavior as a solvent [3–5] and in small confined systems [6, 7]. In work [8], a hierarchy of anomalies in water was proposed: the structural anomalies are observed at temperatures below 360 K, the dynamic anomalies at temperatures below 340 K, and the thermodynamic anomalies at temperatures below 280 K.

Most anomalous properties of water are observed in the temperature interval below 100 °C. For example, the maximum value of the sound propagation speed is observed at a temperature of 74 °C [9], the minimum of isothermal compressibility takes place at a temperature of 46.5 °C [10], that of isobaric heat capacity

Citation: Bulavin L.A., Zabulonov Yu.L., Kopcansky P., Rudnikov Ye.G. Comparative analysis of the temperature dependence of adiabatic thermodynamic coefficients of liquid H_2O, H_2O_2, and Ar. *Ukr. J. Phys.* **70**, No. 2, 99 (2025). https://doi.org/10.15407/ujpe70.2.99.

at a temperature of 36 °C [11], and that of specific volume V at a temperature of 4 °C [12].

The influence of the temperature T, pressure P, and chemical potential μ on the thermodynamic coefficients $-(\partial V/\partial P)_T$ and $(\partial V/\partial T)_P$ of water and argon was studied in our previous works [13, 14]. In work [13], it was shown that the temperatures $T \approx 4$ °C and 42 °C, at which the specific volume V and the isothermal compressibility coefficient $-(\partial V/\partial P)_T$, respectively, of water demonstrate minimum, are correlated with the anomalous phase transition liquid–hexagonal ice $1h$, which is called the entropy-driven phase transition [15, 16].

According to the thermodynamic theory of fluctuations [17], the adiabatic thermodynamic coefficients are related to pressure and temperature fluctuations. According to work [17], the thermodynamic coefficient $-(\partial V/\partial P)_S$ is determined by pressure fluctuations,

$$-(\partial P/\partial V)_S = \frac{\langle(\delta P)^2\rangle}{k_{\rm B}T}, \tag{1}$$

the thermodynamic coefficient $(\partial V/\partial T)_S$ by pressure and temperature fluctuations,

$$(\partial T/\partial V)_S = -(\partial P/\partial S)_V = -\frac{\langle\delta P\delta T\rangle}{k_{\rm B}T}, \tag{2}$$

and the thermodynamic coefficient $(\partial T/\partial P)_S$ by their ratio,

$$(\partial T/\partial P)_S = \frac{(\partial T/\partial V)_S}{(\partial P/\partial V)_S} = \frac{\langle\delta P\delta T\rangle}{\langle(\delta P)^2\rangle}. \tag{3}$$

In our opinion, the study of these quantities is of interest from the viewpoint of finding answers to questions about the physical mechanisms of the anomalous properties of H_2O in the liquid state and the role and character of hydrogen bonds in water.

The aim of this work is to compare the temperature dependences of the adiabatic thermodynamic coefficients $(\partial V/\partial T)_S$, $-(\partial V/\partial P)_S$, and $(\partial T/\partial P)_S$, as well as the related quantity, the speed of sound propagation in liquid H_2O, H_2O_2, and Ar in a vicinity of the liquid-vapor coexistence curve. For the selected objects to study, such a comparison makes it possible to analyze the influence of hydrogen bonds on the indicated adiabatic thermodynamic coefficients of the examined liquids. As is known, there are hydrogen bonds in liquid water H_2O, and they also form a continuous network at normal pressure and in a temperature interval of (0÷42) °C [18]. However, under the same thermodynamic conditions, there are hydrogen bonds in hydrogen peroxide H_2O_2, but they do not form a continuous network [19]. Surely, in liquid argon Ar, there are no hydrogen bonds at all. It is clear that a comparison of these liquids should be carried out on the basis of the principle of corresponding states.

2. Calculation Technique for Adiabatic Thermodynamic Coefficients

When applying the principle of corresponding states [20, 21] to analyze the temperature influence on the adiabatic thermodynamic coefficients $(\partial V/\partial T)_S$, $-(\partial V/\partial P)_S$, $(\partial T/\partial P)_S$, and the related sound velocity C, we used the most reliable data obtained for H_2O [22–24], H_2O_2 [25–27], and Ar [28–30] and published in modern reference books [31, 32] and databases [33–40]. Proceeding from the fact that $_S$, as a rule, the adiabatic thermodynamic coefficients $(\partial V/\partial T)_S$, $-(\partial V/\partial P)_S$, and $(\partial T/\partial P)$ are not measured directly in experiment [32], we calculated those quantities according to the available thermodynamic relationships [17].

The calculations were performed according to the formulas given below (see also work [17]). Then, the thermodynamic coefficient $(\partial V/\partial T)_S$ can be obtained in three ways according to the formulas

$$\left(\frac{\partial V}{\partial T}\right)_S = -\left(\frac{\partial S}{\partial P}\right)_V = \frac{\alpha_P \cdot V}{\left(\frac{C_P}{C_V} - 1\right)} =$$

$$= \frac{\left(\frac{\partial V}{\partial T}\right)_P}{\left(\left(\frac{\partial S}{\partial T}\right)_P \left(\frac{\partial T}{\partial S}\right)_V - 1\right)}, \tag{4}$$

$$\left(\frac{\partial V}{\partial T}\right)_S = \frac{\beta_T \cdot C_V}{T \cdot \alpha_P} = \frac{\left(\frac{\partial V}{\partial P}\right)_T \cdot \left(\frac{\partial S}{\partial T}\right)_V}{\left(\frac{\partial V}{\partial T}\right)_P} \tag{5}$$

or

$$\left|\left(\frac{\partial V}{\partial T}\right)_S\right| = \left(\frac{V \cdot \beta_S}{T\left(\frac{1}{C_V} - \frac{1}{C_P}\right)}\right)^{0.5} =$$

$$= \left(\frac{-\left(\frac{\partial V}{\partial P}\right)_S}{\left(\frac{\partial T}{\partial S}\right)_V - \left(\frac{\partial T}{\partial S}\right)_P}\right)^{0.5}. \tag{6}$$

The thermodynamic coefficient $(\partial T/\partial P)_S$ was obtained as a result of calculations in two ways according to the formulas

$$\left(\frac{\partial T}{\partial P}\right)_S = \left(\frac{\partial V}{\partial S}\right)_P = -\left(\frac{\partial S}{\partial P}\right)_T \cdot \left(\frac{\partial T}{\partial S}\right)_P =$$

$$= \left(\frac{\partial V}{\partial T}\right)_P \cdot \left(\frac{\partial T}{\partial S}\right)_P \tag{7}$$

or

$$\left(\frac{\partial T}{\partial P}\right)_S = \left(\frac{\partial V}{\partial P}\right)_S \cdot \left(\frac{\partial T}{\partial V}\right)_S. \tag{8}$$

In formulas (4)–(8), the following notation was used: the density $\rho = 1/V$, the isobaric heat capacity $C_P = T \cdot (\partial S/\partial T)_P$, the isochoric heat capacity $C_V = T \cdot (\partial S/\partial T)_V$, the isobaric volumetric expansion coefficient $\alpha_P = (\partial V/\partial T)_P/V = -(\partial\rho/\partial T)_P/\rho$, the adiabatic compressibility $\beta_S = -(\partial V/\partial P)_S/V = (\partial\rho/\partial P)_S/\rho$, the isothermal compressibility $\beta_T = -(\partial V/\partial P)_T/V = (\partial\rho/\partial P)_T/\rho$, and the sound propagation speed $C = (\beta_S \cdot \rho)^{-1/2} = (\partial P/\partial\rho)_S^{1/2} = (-(\partial P/\partial V)_S)^{1/2}$. Here, the density $\rho = 1/V$ is measured in kg/m^3 units, and the specific volume V in m^3/kg units.

In order to reduce the error of final results, we used alternative ways (see formulas (4)–(6) and (7)–(8)) when calculating the adiabatic thermodynamic coefficients.

When calculating the sound propagation speed C, the data on the density $\rho = 1/V$ and the adiabatic compressibility $\beta_S = -(\partial V/\partial P)_S/V = (\partial\rho/\partial P)_S/\rho$ were used.

According to the principle of corresponding states, the adiabatic coefficients $(\partial V/\partial T)_S$, $-(\partial V/\partial P)_S$, and $(\partial T/\partial P)_S$ were nondimensionalized using the critical parameter values. In particular, the dimensionless sound propagation speed C^* looks like

$$C^* = \frac{V}{V_C} \cdot \left(-\left(\frac{\partial P}{\partial V}\right)_S \cdot \frac{V_C}{P_C}\right)^{0.5} = \frac{C}{(V_C \cdot P_C)^{0.5}}. \tag{9}$$

The critical parameter values T_C, P_C, and V_C and the freezing temperatures T_M (see Table) were taken from literature databases [31, 32, 39, 40].

3. Temperature Dependences of the Adiabatic Thermodynamic Coefficients of Liquid H_2O, H_2O_2, and Ar in a Vicinity of the Liquid-Vapor Coexistence Curve

3.1. Adiabatic thermal expansion coefficient $(\partial V/\partial T)_S$

Our analysis of the experimental data [32–35] showed that the adiabatic thermal expansion coefficient

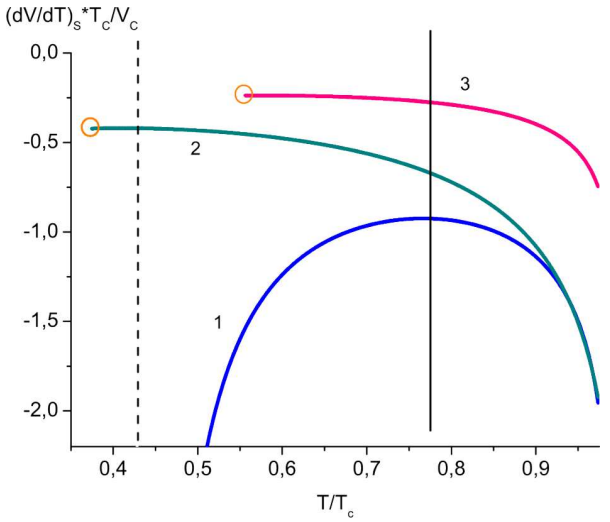

Fig. 1. Temperature dependences of the thermodynamic coefficient $(\partial V/\partial T)_S \cdot T_C/V_C$ along the liquid-vapor coexistence curve for H_2O (*1*), H_2O_2 (*2*), and Ar (*3*). The vertical dashed line marks a temperature of 4 °C characteristic of water. The vertical solid line marks a temperature of 223.1 °C (the maximum of the quantity $(\partial V/\partial T)_S \cdot T_C/V_C$ for H_2O). The circles mark triple points for H_2O_2 and Ar

$(\partial V/\partial T)_S$ is negative [see formula (5)], and it is a monotonically decreasing function of the temperature for most liquids. In Fig. 1, the temperature dependences of the coefficient $(\partial V/\partial T)_S$ for liquid H_2O, H_2O_2, and Ar are shown. Their analysis testifies that, unlike the H_2O case, the temperature dependences of the adiabatic coefficient $(\partial V/\partial T)_S$ for H_2O_2 and Ar are monotonically decreasing function of the temperature within the interval from the triple point to the critical one, and the value of this coefficient remains negative ($(\partial V/\partial T)_S < 0$).

At the same time, for H_2O, $(\partial V/\partial T)_S$ is a nonmonotonic function of the temperature with a maximum at $T = 223.1$ °C. A comparison of these data for H_2O with the data for H_2O_2 and Ar shows that the

Critical temperatures (T_C), critical pressures (P_C), critical specific volumes (V_C), and freezing points (T_M) for H_2O, H_2O_2, and Ar

Liquid	T_M, K	T_C, K	P_C, kPa	V_C, m^3/kg
H_2O	273.16	647.1	22064	0.003106
H_2O_2	272.74	727.98	16202	0.002159
Ar	83.806	150.69	4863	0.001867

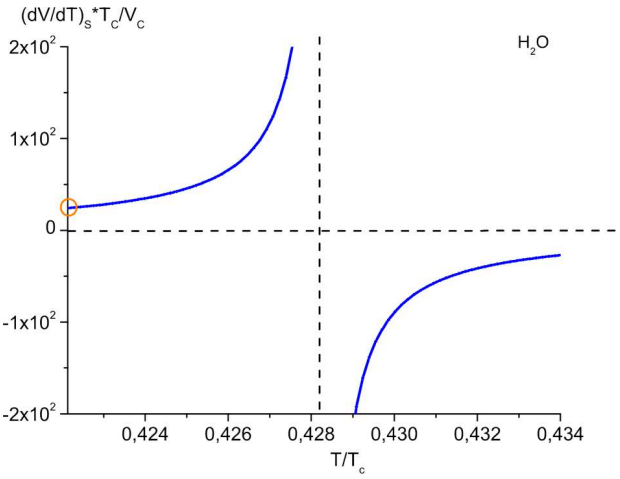

Fig. 2. Temperature dependence of the thermodynamic coefficient $(\partial V/\partial T)_S \cdot T_C/V_C$ along the liquid-vapor coexistence curve for H_2O in the temperature interval $T < 4$ °C. The vertical dashed line marks a characteristic temperature of 4 °C. The triple point is marked with a circle

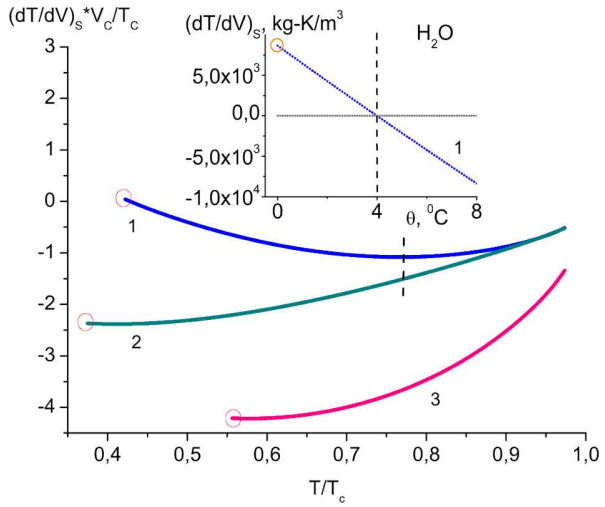

Fig. 3. Temperature dependences of the thermodynamic coefficient $(\partial T/\partial V)_S \cdot V_C/T_C$ along the liquid-vapor coexistence curve for H_2O (*1*), H_2O_2 (*2*), and Ar (*3*). The vertical dashed line marks a temperature of 223.1 °C (the minimum of $(\partial T/\partial V)_S \cdot V_C/T_C$ for H_2O). The circles mark the triple points for H_2O, H_2O_2, and Ar. The temperature dependence of $(\partial T/\partial V)_S$ around 4 °C for H_2O is shown in the unset; the vertical dashed line marks a temperature of 4 °C

principle of corresponding states cannot be applied in a wide temperature interval $T/T_C < 0.8$. Moreover, at relative temperatures $T/T_C > 0.94$, the temperature dependences of $(\partial V/\partial T)_S \cdot T_C/V_C$ for H_2O and

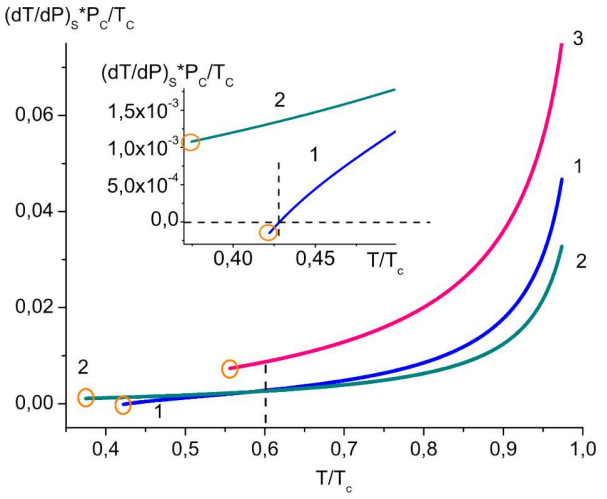

Fig. 4. Temperature dependences of the thermodynamic coefficient $(\partial T/\partial P)_S \cdot P_C/T_C$ along the liquid-vapor coexistence curve for H_2O (*1*), H_2O_2 (*2*), and Ar (*3*). The vertical dashed line marks a temperature of 102.2°C (the inflection point of $(\partial T/\partial P)_S \cdot P_C/T_C$ for H_2O). The inset shows the relative temperature interval $T/T_C < 0.5$. The vertical dashed line marks a temperature of 4 °C (characteristic of H_2O). The circles mark the triple points for H_2O, H_2O_2, and Ar

H_2O_2 practically coincide, differing noticeably from the corresponding dependence for Ar. As follows from Fig. 2, the coefficient $(\partial V/\partial T)_S$ for H_2O has a singularity at a temperature of 4 °C and becomes positive at temperatures $T < 4$ °C, which is not observed for H_2O_2, Ar, and the vast majority of liquids.

Let us consider the temperature dependences of the quantity $(\partial T/\partial V)_S$, which is inverse to the thermodynamic coefficient $(\partial V/\partial T)_S$, for liquid H_2O, H_2O_2, and Ar (see Fig. 3). The corresponding analysis showed that the temperature dependence of $(\partial T/\partial V)_S \cdot V_C/T_C$ for H_2O passes through the zero value at a temperature of 4 °C. For this quantity, the minimum condition $(\partial(\partial V/\partial T)_S)/\partial T)_P = 0$ is satisfied at a temperature of 223.1 °C for H_2O, whereas for H_2O_2 and Ar, this condition is satisfied at their freezing temperatures (0.4097 °C and −189.34 °C, respectively).

3.2. Inverse adiabatic thermal pressure coefficient

Let us consider the adiabatic thermodynamic coefficient $(\partial T/\partial P)_S$, which is the inverse of the adiabatic thermal pressure coefficient $(\partial P/\partial T)_S$. In Fig. 4, the temperature dependences of the dimensionless coeffi-

cient $(\partial T/\partial P)_S \cdot P_C/T_C$ are presented for liquid H_2O, H_2O_2, and Ar. A corresponding analysis showed that the temperature dependence of $(\partial T/\partial P)_S \cdot P_C/T_C$ for H_2O has an inflection point at a temperature of 102.2 °C. The temperature dependence of $(\partial T/\partial P)_S \cdot P_C/T_C$ for H_2O intersects the similar dependence for H_2O_2 and reaches negative values at temperatures $T < 4$ °C.

Unlike H_2O, the temperature dependences of the inverse adiabatic thermal pressure coefficient for H_2O_2 and Ar have no inflection points, being thermodynamically similar to each other.

For H_2O, the temperature dependence of $(\partial T/\partial P)_S$ has an inflection point, reaches negative values below the temperature $T < 4$ °C, and is qualitatively similar to the temperature dependence of $(\partial V/\partial T)_P$ [12]. The inflection point in the $(\partial T/\partial P)_S$ curve at a temperature of 102.2 °C is in mutual relation with a temperature of 4 °C specific for water.

3.3. Thermodynamic coefficient of adiabatic compressibility and speed of sound propagation

Now, let us consider the adiabatic compressibility coefficient $-(\partial V/\partial P)_S$ of liquids. Figure 5 demonstrates the temperature dependences of the dimensionless thermodynamic coefficient of adiabatic compressibility $-(\partial V/\partial P)_T \cdot P_C/V_C$ for H_2O, H_2O_2, and Ar. From the analysis of this figure, it follows that the temperature dependences of $-(\partial V/\partial P)_T \cdot P_C/V_C$ for H_2O_2 and Ar intersect at the relative temperature $T/T_C = 0.94$. In our opinion, the difference between the behaviors of the indicated dependences for H_2O_2 and Ar arise due to the presence of hydrogen bonds in H_2O_2 and their absence in Ar. This difference also demonstrates that the principle of corresponding states is not always obeyed even at high temperatures in a vicinity of the critical point.

For H_2O, the temperature dependence of $-(\partial V/\partial P)_T \cdot P_C/V_C$ has a minimum at 56.3 °C. Above the minimum temperature, the temperature dependence of $-(\partial V/\partial P)_S$ for H_2O is qualitatively similar to its counterparts for H_2O_2 and Ar.

Now, let us consider the speed of sound propagation C^* [Eq. (9)], which is related to the adiabatic compressibility coefficient $-(\partial V/\partial P)_S$. In Fig. 6, the temperature dependences of the sound speed for

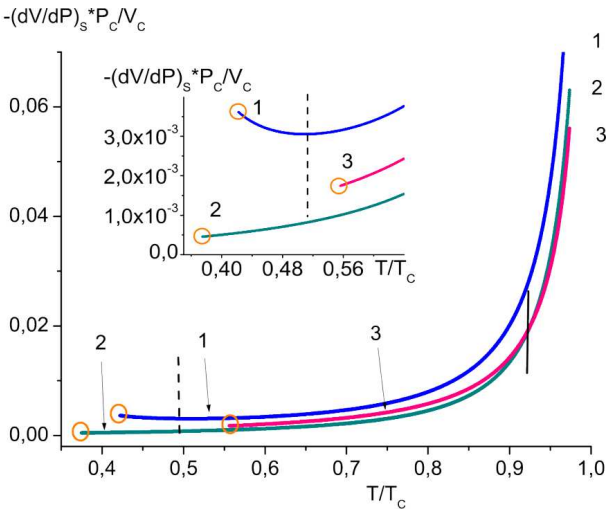

Fig. 5. Temperature dependences of the thermodynamic coefficient $-(\partial V/\partial P)_T \cdot P_C/V_C$ along the liquid-vapor coexistence curve for H_2O (*1*), H_2O_2 (*2*), and Ar (*3*). The inset shows the relative temperature interval $T/T_C < 0.65$. The vertical dashed line marks a temperature of 56.3 °C (the minimum of $-(\partial V/\partial P)_T \cdot P_C/V_C$ for H_2O). The vertical solid line marks the intersection of the $-(\partial V/\partial P)_T \cdot P_C/V_C$ dependences for H_2O_2 and Ar ($T/T_C \approx 0.93$). The circles mark the triple points for H_2O, H_2O_2 and Ar

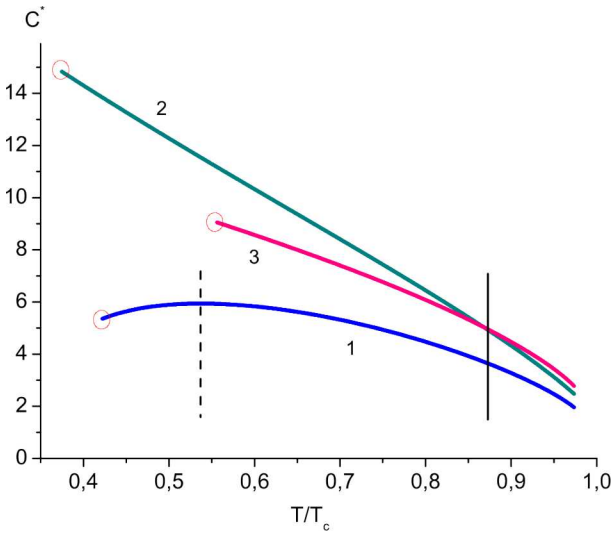

Fig. 6. Temperature dependences of the sound speed C^* along the liquid-vapor coexistence curve for H_2O (*1*), H_2O_2 (*2*), and Ar (*3*). The vertical dashed line marks a temperature of 74.2 °C (the maximum of sound speed in H_2O). The vertical solid line marks the intersection of the C^* dependences for H_2O_2 and Ar ($T/T_C \approx 0.88$). The circles mark the triple points for H_2O, H_2O_2 and Ar

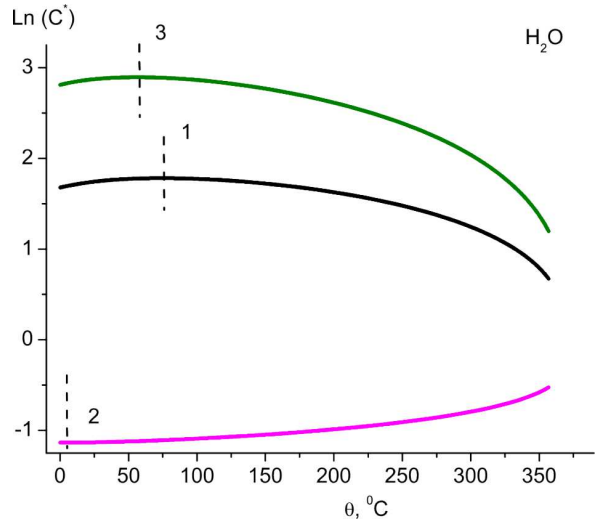

Fig. 7. Temperature dependences of the logarithm of the sound propagation speed (*1*) in H_2O and the logarithmic summands: the specific volume (*2*) and the adiabatic compressibility coefficient (*3*)

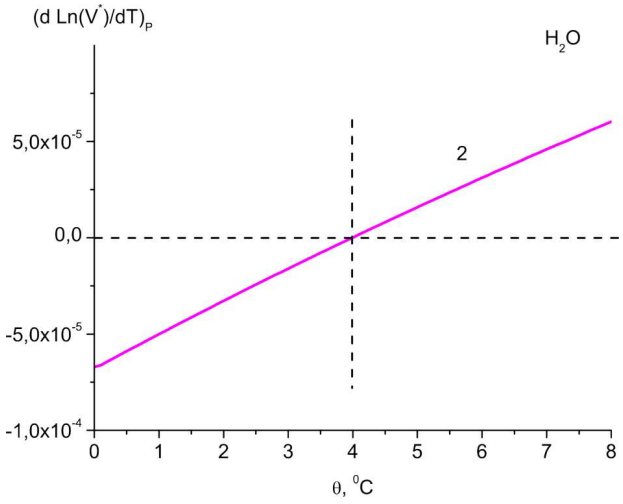

Fig. 8. Temperature dependence of the temperature derivative of the logarithm of the specific volume for H_2O

H_2O, H_2O_2, and Ar nondimensionalized according to Eq. (9) are shown. An analysis of this figure showed that the temperature dependences of the sound speed in H_2O_2 and Ar intersect at the relative temperature $T/T_C \approx 0.88$. This intersection can be a result of the availability of hydrogen bonds in H_2O_2 [19] and their absence in Ar. For H_2O, the temperature dependence of the sound velocity is nonmonotonic and has a minimum at $T = 74.2$ °C.

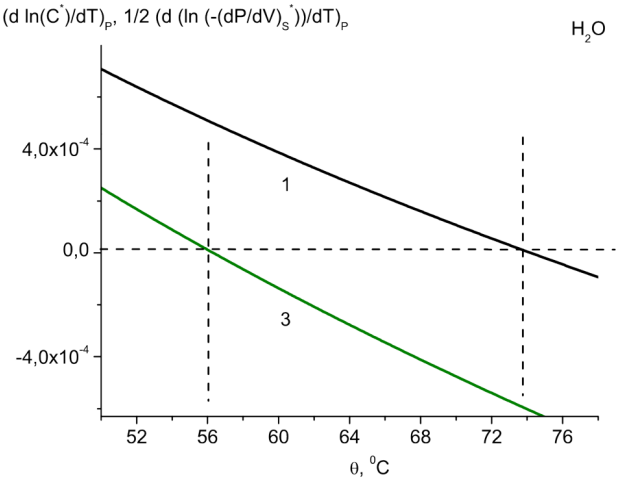

Fig. 9. Temperature dependences of the temperature derivatives of the logarithms of the sound propagation speed (*1*) and the adiabatic compressibility coefficient (*3*) for H_2O

Let us analyze the temperature dependence of the sound speed in the researched liquids. According to formula (9), the dimensionless sound propagation speed C^* depends on the adiabatic compressibility coefficient $-(\partial V/\partial P)_S$ and the specific volume V. To analyze this dependence, we rewrite formula (9) in the logarithmic form,

$$\ln(C^*) = \ln\left(\frac{V}{V_C}\right) + \frac{1}{2}\cdot\ln\left(-\left(\frac{\partial P}{\partial V}\right)_S\cdot\frac{V_C}{P_C}\right) = \\ = \ln(V^*) + \frac{1}{2}\cdot\ln\left(-\left(\frac{\partial P}{\partial V}\right)^*_S\right). \qquad (10)$$

Figure 7 shows the contributions of two terms to the C^*-value for H_2O: from the dimensionless specific volume V^* and the dimensionless adiabatic compressibility coefficient $-(\partial V/\partial P)^*_S$. It follows from Fig. 7 that $\ln(C^*)$ itself and the corresponding contributions to this quantity are nonmonotonic functions of the temperature.

Figures 8 and Fig. 9 illustrate the temperature derivatives of the logarithms of the sound speed, $\ln(C^*)$, and the contributions from the specific volume, $\ln(V/V^*)$, and the adiabatic compressibility coefficient, $\ln(-(\partial P/\partial V)_S\cdot P_C/V_C)^{1/2}$. The intersection of each indicated dependence with the abscissa axis (the zero value of the derivative) determines the temperatures where this dependence has an extremum: at 4.0 °C for the specific volume, at –56.3 °C for the adiabatic compressibility coefficient, and at –74.2 °C

for the speed of sound. As one can see, those extrema are interdependent for H_2O.

4. Discussion

According to the results of neutron research [41, 42], at temperatures below 42 °C and atmospheric pressure, there arises a hydrogen bond network in water. According to the two-structure model [11, 43–45], it is characterized by an enhanced role of the less dense and more ordered structure (the ES structure, the LWD phase) and a reduced role of the more dense and less ordered phase (the CS structure, the HWD phase) [46, 47]. Those water structures are associated in the literature [1, 11, 44] with disordered hydrogen bonds in the rapid picture of their change at the molecular vibration [48–50], flickering [51], and dissociation into H_3O^+ and OH^- ions [52, 53]. The characteristic times of those processes are of an order of 10^{-12} s according to work [52], the change in the water volume at the dissociation of its molecules into ions is maximum at a temperature close to 42 °C.

It should be noted that, in our opinion, such phenomena as the minimum of the isothermal thermodynamic compressibility coefficient $-(\partial V/\partial P)_T$ [54] and the anomalous changes in the viscosity of water [55] and aqueous solutions [56], the pH relaxation time [57, 58], and the Raman depolarization ratio [59] for water, which are observed experimentally, can be considered the signs of the emergence of a hydrogen bond network. At the same time, also in our opinion, the monotonic decrease of $-(\partial V/\partial P)_T$ with the temperature till reaching the triple point, which is observed for other liquids with hydrogen bonds, means that conditions for the emergence of a hydrogen bond network do not arise in them.

In works [19, 60, 61], the H_2O_2 properties were studied, and the hydrogen bonds in H_2O and H_2O_2 were compared. According to the results of those works, the strength of hydrogen bonds in H_2O_2 is weaker than that in H_2O. The maximum number of possible hydrogen bonds for a H_2O_2 molecule equals six, which is larger than that for H_2O. The self-diffusion coefficient of hydrogen peroxide is approximately equal to half the self-diffusion coefficient of water [61]. The addition of hydrogen peroxide to water destroys the tetrahedral network structure of hydrogen bonds in water [61]. Although the freezing points of H_2O_2 and H_2O are close, the boiling point of H_2O_2 is noticeably higher than that of H_2O. Unlike the first-order phase transition liquid-hexagonal ice in H_2O, the density of H_2O_2 in the solid state exceeds its density in the liquid phase at the first-order liquid-solid phase transition [62]. These properties mean that, unlike the anomalous entropy-driven phase transition in H_2O [14–16], the phase transition in H_2O_2 has the features of a density-driven one [63].

It can be assumed that, in this case, there are no factors for the growth of the role of the more expanded, but also more ordered, structure in H_2O_2. This assumption is supported by thermodynamic experimental data [32–35, 39] according to which, the minimum of the quantity $-(\partial V/\partial P)_T$ along the liquid-vapor coexistence curve is not observed for H_2O_2, in contrast to H_2O.

5. Conclusions

1. The temperature dependences of the adiabatic thermodynamic coefficients for water, where a hydrogen bond network is formed under certain conditions, hydrogen peroxide, where hydrogen bonds exist, but do not form a network, and argon, where hydrogen bonds are absent altogether, were compared.

2. It was shown that, unlike the cases of argon and hydrogen peroxide, the thermodynamic coefficient $(\partial V/\partial T)_S$ for H_2O diverges at a temperature of 4 °C and becomes positive in the temperature interval $T < 4$ °C; the thermodynamic coefficient $(\partial T/\partial P)_S$ has an inflection point at a temperature of 102.2 °C and reaches zero at a temperature of 4 °C specific for water and negative values at temperatures below 4 °C; the thermodynamic coefficient $-(\partial V/\partial P)_S$ has a minimum at a temperature of 56.3 °C.

3. In our opinion, the temperature dependences of the adiabatic thermodynamic coefficients of water originate from the existence of a hydrogen bond network, which is formed by two dynamic structures.

4. It is shown that, unlike the case of argon, for hydrogen peroxide, where hydrogen bonds also exist, but there is no hydrogen bond network, the temperature dependences of the quantity $(\partial V/\partial P)_S \cdot T_C/V_C$ at temperatures $T/T_C > 0.93$ coincide with similar dependences for water.

5. It is shown that the hydrogen bond network in water substantially affects the character of the temperature dependence of the sound propagation speed, which is related to the adiabatic compressibility coef-

ficient. For argon and hydrogen peroxide, this dependence is monotonic, but, for water, it has a minimum at a temperature of 74.2 °C.

This research was partially supported in the framework of the projects No. APVV-22-0060 MAMOTEX and ITMS 313011T548 MODEX (Slovak Research and Development Agency, Ministry of Education, Science, Research and Youth of the Slovak Republic).

1. L.G.M. Pettersson. A two-state picture of water and the funnel of life. In: *Modern Problems of the Physics of Liquid Systems. PLMMP 2018*. Edited by L. Bulavin, L. Xu (Springer, 2019), p. 3.
2. M. F. Chaplin. Structure and properties of water in its various states. In: *Encyclopedia of Water: Science, Technology, and Society*. Edited by P.A. Maurice (Wiley, 2019), p. 1.
3. A. Oleinikova, L. Bulavin, V. Pipich. Critical anomaly of shear viscosity in a mixture with an ionic impurity. *Chem. Phys. Lett.* **278**, 121 (1997).
4. V.F. Korolovych, A. Erwin, A. Stryutsky, H. Lee, W.T. Heller, V.V. Shevchenko, L.A. Bulavin, V.V. Tsukruk. Thermally responsive hyperbranched poly(ionic liquid)s. *Assemb. Phase Transform. Macromol.* **51**, 4923 (2018).
5. I. Safarik, J. Prochazkova, M.A. Schroer, V.M. Garamus, P. Kopcansky; M. Timko, M. Rajnak, M. Karpets, O.I. Ivankov, M.V. Avdeev, V.I. Petrenko, L. Bulavin, K. Pospiskova. Cotton textile/iron oxide nanozyme composites with peroxidase-like activity: Preparation, characterization, and application. *ACS Appl. Mater. Interfac.* **13**, 23627 (2021).
6. L.A. Bulavin, V.F. Chekhun, A.A. Vasilkevich, V.I. Kovalchuk, V.T. Krotenko, V.I. Slisenko, V.P. Trindyak, K.A. Chalyy, S.D. Galyant. Neutron investigations of self-diffusion of water molecules in plasmatic membranes. *J. Phys. Stud.* **8**, 334 (2004).
7. K.A. Chalyy, L.A. Bulavin, V.F. Chekhun, A.V. Chalyi, Y.V. Tsekhmister, L.M. Chernenko. Fundamentals and medical applications of neutron and light spectroscopy of confined liquids. *IFMBE Proc.* **25**, N 13, 197 (2009).
8. J.R. Errington, P.G. Debenedetti. Relationship between structural order and the anomalies of liquid water. *Nature* **409**, 318 (2001).
9. G. Venktaramana, E. Rajagopal, N. Manohara Murthy. Studies on the effect of chlorides of magnesium, calcium, strontium and barium on the temperature of the sound velocity maximum of water. *J. Mol. Liq.* **123**, 68 (2006).
10. L.N. Dzhavadov, V.V. Brazhkin, Y.D. Fomin, V.N. Ryzhov, E.N. Tsiok. Experimental study of water thermodynamics up to 1.2 GPa and 473 K. *J. Chem. Phys.* **152**, 154501 (2020).
11. R.C. Dougherty, L.N. Howard. Equilibrium structural model of liquid water: Evidence from heat capacity, spectra, density, and other properties. *J. Chem. Phys.* **109**, 7379 (1998).
12. P. Gallo, K. Amann-Winkel, Ch.A. Angell, M.A. Anisimov, F. Caupin, Ch. Chakravarty, E. Lascaris, T. Loerting, A.Z. Panagiotopoulos, J. Russo, J.A. Sellberg, H.E. Stanley, H. Tanaka, C. Vega, L. Xu, L.G.M. Pettersson. Water: A tale of two liquids. *Chem. Rev.* **116**, 7463 (2016).
13. L.A. Bulavin , E.G. Rudnikov. Temperature and pressure effect on the thermodynamics coefficient $(\partial V/\partial T)_P$ of water. *Ukr. J. Phys.* **68**, 122 (2023).
14. L.A. Bulavin, E.G. Rudnikov. The influence of the temperature and chemical potential on the thermodynamic coefficient $-(\partial V/\partial P)_T$ of water. *Ukr. J. Phys.* **68**, 390 (2023).
15. V. Holten, M.A. Anisimov. Entropy-driven liquid–liquid separation in supercooled water. *Sci. Rep.* **2**, 713 (2012).
16. V. Holten, J.C. Palmer, P.H. Poole, P.G. Debenedetti, M.A. Anisimov. Two-state thermodynamics of the ST2 model for supercooled water. *J. Chem. Phys.* **140**, 104502 (2014).
17. L.D. Landau, E.M. Lifshitz. *Statistical Physics. Course of Theoretical Physics. Vol. 5* (Elsevier, 1980).
18. L.A. Bulavin, T.V. Lokotosh, N.P. Malomuzh. Role of the collective selfdiffusion in water and other liquids. *J. Mol. Liq.* **137**, 1 (2008).
19. P.A. Giguère, Hung Chen. Hydrogen bonding in hydrogen peroxide and water. A Raman study of the liquid state. *J. Raman Spectrosc.* **15**, 199 (1984).
20. I.I. Novikov. Thermodynamic similarity and prediction of the properties and characteristics of substances and processes. *J. Eng. Phys. Fundam. Thermodyn.* **53**, 1227 (1987).
21. H.W. Xiang. *The Corresponding-States Principle and Its Practice. Thermodynamic, Transport and Surface Properties of Fluids* (Elsevier Science, 2005) [ISBN: 0444520627].
22. A. Saul, W. Wagner. A fundamental equation for water covering the range from the melting line to 1273 K at pressures up to 25000 MPa. *J. Phys. Chem. Ref. Data* **18**, 1537 (1989).
23. W. Wagner, A. Pruss. The IAPWS formulation 1995 for the thermodynamic properties of ordinary water substance for general and scientific use. *J. Phys. Chem. Ref. Data* **31**, 387 (2002).
24. O. Kunz, R. Klimeck, W. Wagner, M. Jaeschke. *The GERG-2004 Wide-Range Equation of State for Natural Gases and Other Mixtures* (Fortschritt-Berichte VDI, 2007).
25. O. Maass, P.G. Hiebert. The properties of pure hydrogen peroxide. V. Vapor pressure. *J. Am. Chem. Soc.* **46**, 2693 (1924).
26. A.C. Cuthbertson, G.L. Matheson, O. Maass. The freezing point and density of pure hydrogen peroxide. *J. Am. Chem. Soc.* **50**, 1120 (1928).
27. E.D. Nikitin, P.A. Pavlov, A.P. Popov, H.E. Nikitina. Critical properties of hydrogen peroxide determined from direct measurements. *J. Chem. Thermodyn.* **27**, 945 (1995).
28. B.A. Younglove. Thermophysical properties of fluids. I. Argon, ethylene, parahydrogen, nitrogen, nitrogen trifluoride, and oxygen. *J. Phys. Chem. Ref. Data* **11**, 1 (1982) [ISBN: 088318415X].

29. R.B. Stewart, R.T. Jacobsen. Thermodynamic properties of argon from the triple point to 1200 K at pressures to 1000 MPa. *J. Phys. Chem. Ref. Data* **18**, 639 (1989).
30. Ch. Tegeler, R. Span, W. Wagner. A new equation of state for argon covering the fluid region for temperatures from the melting line to 700 K at pressures up to 1000 MPa. *J. Phys. Chem. Ref. Data* **28**, 779 (1999).
31. C. Yaws. *Thermophysical Properties of Chemicals and Hydrocarbons. Second Edition* (Gulf Professional Publishing, 2014).
32. M.Z. Southard, D.W. Green. *Perry's Chemical Engineers' Handbook* (Mcgraw-Hill Education, 2019).
33. *SRD69 Database, Thermophysical Properties of Fluid Systems, Peter Linstrom (2017), NIST Chemistry WebBook – SRD 69* (National Institute of Standards and Technology, 2017); accessed 2023-04-20, https://webbook.nist.gov/chemistry/fluid.
34. *MiniRefprop Database, NIST*. https://trc.nist.gov/refprop/MINIREF/MINIREF.HTM.
35. I.H. Bell, J. Wronski, S. Quoilin, V. Lemort. Pure and pseudo-pure fluid thermophysical property evaluation and the open-source thermophysical property library CoolProp. *Ind. Eng. Chem. Res.* **53**, 2498 (2014).
36. *Refprop Database, NIST*. https://www.nist.gov/programs-projects/reference-fluid-thermodynamic-and-transport-properties-database-refprop.
37. *ThermodataEngine Database, NIST*. https://trc.nist.gov/tde.html.
38. *WTT Database, NIST*. https://wtt-pro.nist.gov/wtt-pro/.
39. *MOL-Instincts Database, ChemEssen*. https://www.molinstincts.com/(0001-iyf6; 0001-ixac).
40. *ChemRTP Database, ChemEssen*. http://www.chemrtp.com/(XLYOFNOQVPJJNP-UHFFFAOYSA-N; MHAJPDPJQMAIIY-UHFFFAOYSA-N).
41. J. Teixeira, M.-C. Bellissent-Funel, S.-H. Chen, J. Dianoux. Experimental determination of the nature of diffusive motions of water molecules at low temperatures. *Phys. Rev. A* **31**, 1913 (1985).
42. J. Teixeira, J.-M. Zanotti, M.-C. Bellissent-Funel, S.-H. Chen. Water in confined geometries. *Physica B* **234–236**, 370 (1997).
43. J. Russo, H. Tanaka. Understanding water's anomalies with locally favoured structures. *Nat. Commun.* **5**, 3556 (2014).
44. A. Nilsson, L.G.M. Pettersson. The structural origin of anomalous properties of liquid water. *Nat. Commun.* **6** (1), 8998 (2015).
45. R. Shi, H. Tanaka. Direct evidence in the scattering function for the coexistence of two types of local structures in liquid water. *J. Am. Chem. Soc.* **142**, 2868 (2020).
46. A. Kholmanskiy, N. Zaytseva. Physically adequate approximations for abnormal temperature dependences of water characteristics. *J. Mol. Liq.* **275**, 741 (2019).
47. A Kholmanskiy. Hydrogen bonds and dynamics of liquid water and alcohols. *J. Mol. Liq.* **325**, 115237 (2021).
48. T. Seki, K.-Y. Chiang, C.-C. Yu, X. Yu, M. Okuno, J. Hunger, Y. Nagata, M. Bonn. The bending mode of water: A powerful probe for hydrogen bond structure of aqueous systems. *J. Phys. Chem. Lett.* **11**, 8459 (2020).
49. H. Zhao, Y. Tan, L. Zhang, R. Zhang, M. Shalaby, C. Zhang, Y. Zhao, X.-Ch. Zhang. Ultrafast hydrogen bond dynamics of liquid water revealed by terahertz-induced transient birefringence. *Light Sci. Appl.* **9**, 136 (2020).
50. J. Yang, R. Dettori, J.P.F. Nunes, N.H. List, E. Biasin, M. Centurion, Zh. Chen, A.A. Cordones, D.P. Deponte, T.F. Heinz, M.E. Kozina, K. Ledbetter, M.-Fu Lin, A.M. Lindenberg, M. Mo, A. Nilsson, X. Shen, T.J.A. Wolf, D. Donadio, K.J. Gaffney, T.J. Martinez, X. Wang. Direct observation of ultrafast hydrogen bond strengthening in liquid water. *Nature* **596**, 531 (2021).
51. Z.A. Piskulich, D. Laage, W.H. Thompson. Activation energies and the extended jump model: How temperature affects reorientation and hydrogen-bond exchange dynamics in water. *J. Chem. Phys.* **153**, 074110 (2020).
52. Y. Marcus. Volumes of aqueous hydrogen and hydroxide ions at 0 to 200 °C. *J. Chem. Phys.* **137**, 154501 (2012).
53. N.P. Malomuzh, O. Khorolskyi. Structure and properties of the hydroxonium ion. *Chem. Phys. Lett.* **858**, 141743 (2025).
54. L.A. Bulavin, E.G. Rudnikov, A.V. Chalyi. Thermodynamic anomalies of water near its singular temperature of 42 °C. *J. Mol. Liq.* **389**, 122849 (2023).
55. L.A. Bulavin, A.I. Fisenko, N.P. Malomuzh. Surprising properties of the kinematic shear viscosity of water. *Chem. Phys. Lett.* **453**, 183 (2008).
56. M.M. Lazarenko, O.M. Alekseev, S.G. Nedilko, A.O. Sobchuk, V.I. Kovalchuk, S.V. Gryn, V.P. Scherbatskyi, S.Yu. Tkachev, D.A. Andrusenko, E.G. Rudnikov, A.V. Brytan, K.S. Yablochkova, E.A. Lysenkov, R.V. Dinzhos, S. Thomas, T. Rose Abraham. Impact of the alkali metals ions on the dielectric relaxation and phase transitions in water solutions of the hydroxypropylcellulose. In: *Nanoelectronics, Nanooptics, Nanochemistry and Nanobiotechnology, and Their Applications. NANO 2022* (Springer, 2022), p. 37.
57. L.A. Bulavin, N.P. Malomuzh, O.V. Khorolskyi. Temperature and concentration dependences of pH in aqueous NaCl solutions with dissolved atmospheric CO_2. *Ukr. J. Phys.* **67**, 833 (2022).
58. O. Khorolskyi, A. Kryvoruchko. Non-trivial behavior of the acid-base balance of pure water near the temperature of its dynamic phase transition. *Ukr. J. Phys.* **66**, 972 (2021).
59. N.K. Alphonse, S.R. Dillon, R.C. Dougherty, D.K. Galligan, L.N. Howard. Direct Raman evidence for a weak continuous phase transition in liquid water. *J. Phys. Chem. A* **110**, 7577 (2006).
60. Chun-Yang Yu, Zhong-Zhi Yang. A systemic investigation of hydrogen peroxide clusters $(H_2O_2)_n$ (n = 1–6) and liquid-state hydrogen peroxide: Based on atom-bond electronegativity equalization method fused into molecular mechanics and molecular dynamics. *J. Phys. Chem. A* **115**, 2615 (2011).
61. C. Parida, S. Chowdhuri. Effects of hydrogen peroxide on the hydrogen bonding structure and dynamics of water and its influence on the aqueous solvation of insulin monomer. *J. Phys. Chem. B* **127**, 10814 (2023).

62. S.C. Abrahams, R.L. Collin, W.N. Lipscomb. The crystal structure of hydrogen peroxide. *Acta Cryst.* **4**, 15 (1951).
63. M. Seidl, A. Fayter, J.N. Stern, K. Amann-Winkel, M. Bauer, T. Loerting. High-performance dilatometry under extreme conditions. *Proc. 6th Zwick Academia Day* (2015) (Zwick GmbH & Co. KG, 2015).

Received 21.11.24.
Translated from Ukrainian by O.I. Voitenko

Л.А. Булавін, Ю.Л. Забулонов,
П. Копчанський, Є.Г. Рудніков

ПОРІВНЯЛЬНИЙ АНАЛІЗ ТЕМПЕРАТУРНОЇ ЗАЛЕЖНОСТІ АДІАБАТИЧНИХ ТЕРМОДИНАМІЧНИХ КОЕФІЦІЄНТІВ ДЛЯ H_2O, H_2O_2, Ar У СТАНІ РІДИНИ

Проведено порівняння температурних залежностей адіабатичних термодинамічних коефіцієнтів води, у якій за певних умов утворюється сітка водневих зв'язків, з відповідними залежностями для перекису водню, в якому існують водневі зв'язки, але сітка водневих зв'язків не утворюється, та з аргоном, в якому водневі зв'язки взагалі відсутні. Особливі температурні залежності адіабатичних термодинамічних коефіцієнтів води, на нашу думку, пов'язані з існуванням у воді за певних умов сітки водневих зв'язків, які утворюються двома динамічними структурами (LWD та HDW фази), що зумовлює ієрархію аномальних властивостей води у широкому інтервалі температур. Крім того, показано, що сітка водневих зв'язків суттєво впливає на характер температурних залежностей швидкості поширення звуку, яка пов'язана із адіабатичним коефіцієнтом стисливості рідини.

Ключові слова: вода, аргон, перекис водню, адіабатичний коефіцієнт стисливості, швидкість звуку, водневі зв'язки.